Journal of Engineering Mathematics 19 (1985) 297–319.
© 1985 Martinus Nijhoff Publishers, Dordrecht. Printed in The Netherlands.

Diffraction of water waves by a moored, horizontal, flat plate

M. McIVER *

School of Mathematics, University of Bristol, University Walk, Bristol BS8 1TW, UK

(Received April 10, 1985)

Summary

A Norwegian research group has investigated the feasibility of constructing a system of underwater structures which would act like a lens and focus water waves prior to harnessing their energy. In the present work we consider modelling one of these structures by a horizontal, flat plate which is moored to the seabed. The water is assumed to be incompressible and inviscid and two-dimensional, linear, irrotational theory is used. Solutions to the scattering and radiation potentials are obtained by the method of matched eigenfunction expansions. Comparisons are made with various approximate solutions and results are presented illustrating the effect of varying the mooring stiffness in the cables on both the responses of the plate and the far-field wave motion.

1. Introduction

The possibility of performing large-scale, cost-effective extraction of energy from the ocean waves has received considerable attention over the last two decades, motivated, no doubt, by the desire to obtain a clean, renewable energy source (see Evans [3] for a review of the theoretical aspects of the subject). In particular, a Norwegian research group has investigated the feasibility of constructing a system of underwater structures that would act like a lens and focus waves prior to harnessing their energy (Mehlum and Stamnes [9]). Such a lens system would operate under the same principles that govern the focussing of light waves. As a wave enters the shallower region over a submerged body, the wavelength is decreased and, as is well-known, the wave speed is reduced. Thus, a phase lag is induced in the transmitted wave on the far side of the body. A water-wave lens would be constructed out of several submerged bodies, each of which is capable of retarding a wave by a different amount.

Each lens element must clearly possess the property that it reflects very little of the incident wave, over a wide range of wave frequencies and directions. A notable candidate for such an element is the submerged circular cylinder (Dean [2], Ursell [17]), which is transparent to normally incident waves of all frequencies, and this has indeed considered by Mehlum [8]. Total transmission of normally incident waves past other bodies does also occur but in general, only at isolated frequencies. Examples of bodies that fall into this category are long, two-dimensional objects (Newman [12]) and bodies of rectangular cross-section placed on the seabed (Mei and Black [11]).

* Present address: Department of Mathematics, University College London, London WC1E 6BT, UK.

In addition, as the lens element would doubtless be moored in some way, it is necessary to determine how the reflection and transmission coefficients are affected by the motion of the element. It is also desirable, for cost purposes, that the elements should not be too bulky. In the present work, full linear theory is used to investigate the transmission of surface waves normally incident on a submerged, horizontal plate which is moored to the seabed.

The scattering of waves, obliquely incident on a fixed, horizontal, thin plate of semi-infinite extent, was first studied by Heins [7] using a method based on the Wiener-Hopf technique. His formulation enables the reflection and transmission coefficients to be given explicitly and simply, thus providing a valuable check, using a long-body approximation, on the results for the fixed, finite plate. The Wiener-Hopf technique was used again by Burke [1] for the finite, horizontal plate in infinitely deep water. He obtained, as a limiting case, the results of Greene and Heins [5] for the semi-infinite plate in infinitely deep water. More recently, Patarapanich [13] has investigated the scattering of waves by a fixed, submerged, horizontal plate using a shallow-water approximation developed by Siew and Hurley [15]. He observed a marked oscillatory behaviour in the reflection coefficient, which he investigated by considering the energy flux around the plate. Zeros of reflection from a fixed plate which is deeply submerged were also observed by Grue and Palm [6] in their investigation of reflection of surface waves by submerged cylinders of various cross-sections. In a second paper [14] Patarapanich evaluated the force and moment on a fixed plate using a finite-element technique. This technique which may be used to solve for the flow round a wide class of geometries has the disadvantage that it can be computationally expensive to implement. In the present work, we prefer to use the method of matched eigenfunction expansions (see, for example, Evans and McIver [4]) which is particularly suitable for rectangular geometries.

The problem considered here is that of waves normally incident on a thin, horizontal plate of finite width which is submerged under the free surface and attached to the seabed by four vertical, elastic cables, symmetrically placed around the plate, as illustrated in Figure 1. As a first approximation, it is assumed that two-dimensional motion only need be considered as if, for example, the plate were in a narrow wave tank. It is also assumed that the presence of the cables does not affect the wave field. Linear theory is used, so that the velocity potential may be split into two fundamental parts: one due to the scattering of waves by the fixed plate and the other due to the radiation of waves by the moving plate into otherwise calm water. The full solution to both the scattering and radiation potentials is obtained by the method of matched eigenfunction expansions.

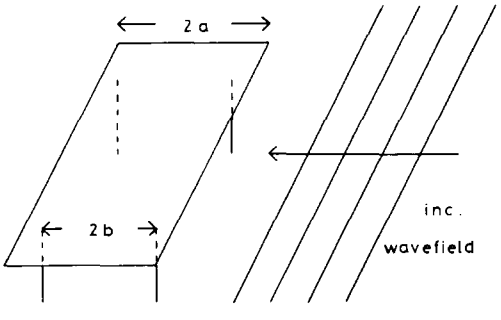

Figure 1. Definition sketch.

The problem is formulated in Section 2 where the usual linearised equations and boundary conditions to be satisfied by the scattering and radiation potentials are presented, on the assumptions of an inviscid, incompressible fluid and irrotational flow. The equations of motion of the plate are derived that determine its amplitude of oscillation in each mode of motion. In Section 3 the method of matched eigenfunction expansions is discussed and the solution for the scattering potential is given in detail. The modifications needed to solve for the radiation potential are also presented. Two systems of equations arise out of the matching and their numerical solution is described in Section 4.

In Section 5 results are presented that illustrate the variation of the reflection coefficient from a fixed plate with wave frequency for a variety of plate widths and submergence depths. Comparisons are made with the results from a long-body approximation and also with the shallow-water results. In order to assess the importance of the energy flux above and below the plate, the full linear results are compared with those for a rectangular block on the seabed with the same height and width as the plate and a rectangular block on the surface with the same depth and width as the plate. For consistency, both these secondary problems are solved using the method of matched eigenfuction expansions although results based on a variational approximation are available in Mei and Black [11]. The influence of the plate motion on the wave field at large distances is discussed and results presented illustrating the effect of varying the mooring stiffness of the cables on both the responses of the plate and the amplitude and phase of the far-field wave motion.

2. Formulation

A two-dimensional cross-section through the plate is illustrated in Figure 2. Cartesian axes are chosen with the x-axis along the mean free surface and the y-axis pointing vertically downwards. The total depth of the water is denoted by h_1 and the depth of submergence of the plate by h_2. The ends of the plate are at $x = \pm a$.

The water is assumed to be incompressible and inviscid. Two-dimensional, linear, irrotational theory is used, so the motion may be described by a velocity potential, Φ, which is written as

$$\Phi = \mathrm{Re}\left[(\phi_s + \phi_r)\, \mathrm{e}^{-\mathrm{i}\omega t}\right] \tag{2.1}$$

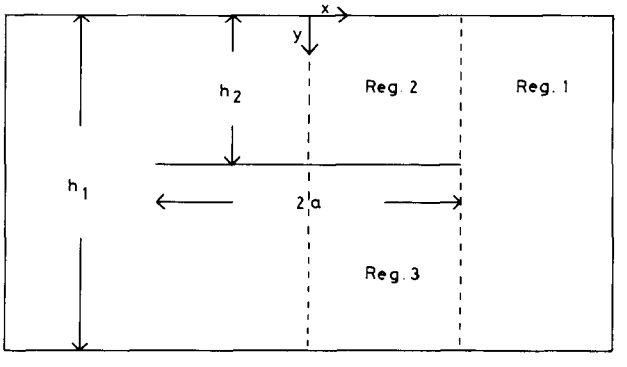

Figure 2. Regions of separate eigenfunction expansions.

after making the further requirement that the motion be periodic in time, with period $2\pi/\omega$.

The scattering potential, ϕ_s, satisfies

$$\nabla^2\phi_s = 0 \quad \text{in the fluid} \tag{2.2}$$

with the boundary conditions

$$\kappa\phi_s + \frac{\partial\phi_s}{\partial y} = 0 \quad \text{on} \quad y = 0, \tag{2.3}$$

where

$$\kappa = \omega^2/g; \tag{2.4}$$

$$\frac{\partial\phi_s}{\partial y} = 0 \quad \text{on} \quad y = h_1, \tag{2.5}$$

$$\frac{\partial\phi_s}{\partial y} = 0 \quad \text{on} \quad y = h_2, \ -a \leqslant x \leqslant a, \tag{2.6}$$

and

$$\phi_s \quad \text{and} \quad \frac{\partial\phi_s}{\partial x} \quad \text{are continuous on} \quad x = \pm a, \tag{2.7}$$

ensuring continuity of pressure and fluid velocity on $x = \pm a$.

For a wave of amplitude A, incident on the plate from $x = \pm\infty$, the radiation condition

$$\phi_s \sim \begin{cases} \phi_0 \cosh k_1(y - h_1)[e^{-ik_1x} + Re^{ik_1x}] & \text{as } x \to \infty \\ \phi_0 T \cosh k_1(y - h_1)\, e^{-ik_1x} & \text{as } x \to -\infty \end{cases} \tag{2.8}$$

must be satisfied, where

$$\phi_0 = \frac{-i\omega A}{k_1 \sinh k_1 h_1} \tag{2.9}$$

and k_1h_1 is the only real, positive root of the equation

$$\kappa h_1 = k_1 h_1 \tanh k_1 h_1. \tag{2.10}$$

The quantities R and T are the reflection and transmission coefficients, respectively.

Using linearity, the radiation potential, ϕ_r, is conventionally written as the sum of separate potentials, each of which is due to the plate moving in one of its modes of motion. Under the assumptions made, the only possible modes of motion of the plate are parallel to the y-axis, heave motion, and about what would be the z-axis, roll motion. Thus

$$\phi_r = -i\omega\eta_3\phi_3 - i\omega\eta_5\phi_5, \tag{2.11}$$

where

$$\zeta_\alpha = \mathrm{Re}\left[\eta_\alpha \, \mathrm{e}^{-\mathrm{i}\omega t}\right], \quad \alpha = 3, 5, \tag{2.12}$$

is the plate motion in the α-direction, and heave and roll motion are denoted by $\alpha = 3$ and 5, respectively.

The potentials ϕ_3 and ϕ_5 satisfy equations (2.2)–(2.5) and (2.7). The body boundary condition (2.6) is replaced by

$$\frac{\partial \phi_3}{\partial y} = 1 \quad \text{on} \quad y = h_2, \; -a \leqslant x \leqslant a, \tag{2.13}$$

and

$$\frac{\partial \phi_5}{\partial y} = x \quad \text{on} \quad y = h_2, \; -a \leqslant x \leqslant a. \tag{2.14}$$

The far-field behaviour of the potentials is governed by

$$\phi_\alpha \sim \frac{-\mathrm{i}\omega A_\alpha^{\pm}}{k_1 \sinh k_1 h_1} \cosh k_1 (y - h_1) \, \mathrm{e}^{\mathrm{i}k_1 |x|} \quad \text{as} \quad x \to \pm\infty, \; \alpha = 3, 5. \tag{2.15}$$

The displacement amplitudes η_α are determined from the equations of motion of the plate. On account of the symmetry of the plate and mooring system, there is no coupling between heave and roll and the equations of motion are given by

$$m_\alpha \ddot{\zeta}_\alpha = -c_\alpha \zeta_\alpha + F_\alpha^e + F_\alpha^r, \quad \alpha = 3, 5, \tag{2.16}$$

where m_3 is the mass per unit length of the plate and m_5 the moment of inertia about the midpoint $= m_3 a^2/3$; c_3 is the net mooring stiffness per unit length and $c_5 = c_3 b^2$, where b is the distance between the point of cable attachment to the plate and the midpoint of the plate as defined in Figure 1; F_α^e is the exciting force or moment per unit length in the α-direction due to the waves scattered by the fixed plate; F_α^r is the radiation force or moment per unit length in the α-direction due to the motion of the plate. Conventionally, F_α^r is split into a component in phase with the velocity and a component in phase with the acceleration of the plate in the α-direction. Thus,

$$F_\alpha^r = -a_\alpha \ddot{\zeta}_\alpha - b_\alpha \dot{\zeta}_\alpha, \tag{2.17}$$

where a_α and b_α are the added-mass and damping coefficients respectively. Removal of the time dependence from (2.16) by writing

$$F_\alpha^e = \mathrm{Re}\left[\chi_\alpha \, \mathrm{e}^{-\mathrm{i}\omega t}\right] \tag{2.18}$$

and using (2.12) yields the following formula for the displacement amplitudes:

$$\eta_\alpha = \frac{\chi_\alpha}{c_\alpha - \omega^2 (m_\alpha + a_\alpha) + \mathrm{i}\omega b_\alpha}. \tag{2.19}$$

3. Method of solution

Only the procedure for solving for ϕ_s will be given in detail, as that for ϕ_r follows in an analogous manner.

The symmetry of the problem is exploited by splitting ϕ_s into symmetric and antisymmetric parts. Thus

$$\phi_s(x, y) = \phi^s(x, y) + \phi^a(x, y) \tag{3.1}$$

where

$$\phi^s(-x, y) = \phi^s(x, y), \quad \frac{\partial \phi^s}{\partial x} = 0 \qquad \text{on} \quad x = 0, \tag{3.2}$$

and

$$\phi^a(-x, y) = -\phi^a(x, y), \quad \phi^a = 0 \qquad \text{on} \quad x = 0. \tag{3.3}$$

The fluid in the domain $x \geqslant 0$ is divided into three regions as illustrated in Figure 2. Region 1 is defined by $x \geqslant a$, $0 \leqslant y \leqslant h_1$, region 2 by $x \leqslant a$, $0 \leqslant y \leqslant h_2$ and region 3 by $x \leqslant a$, $h_2 \leqslant y \leqslant h_1$.

Complete sets of orthonormal eigenfunctions appropriate to each region and satisfying the boundary conditions given in (3.2), (2.5) and (2.6), are constructed (see e.g. Wehausen and Laitone [18], §16). The eigenfunctions appropriate to regions 1 or 2 are defined by

$$\psi_{in} = \frac{\cos k_{in}(y - h_i)}{N_{in}}, \quad i = 1, 2, \quad n = 0, 1, 2, \ldots, \tag{3.4}$$

where $k_{in}h_i$ $(i = 1, 2, n > 0)$ are the two infinite sequences of positive roots, taken in ascending order of magnitude, of the equations

$$\kappa h_i = -k_{in}h_i \tan k_{in}h_i. \tag{3.5}$$

The quantities k_{i0} $(i = 1, 2)$ are imaginary and defined by

$$k_{i0} = -\mathrm{i}k_i \tag{3.6}$$

where k_ih_i are the only positive roots of the equations

$$\kappa h_i = k_ih_i \tanh k_ih_i, \quad i = 1, 2. \tag{3.7}$$

The eigenfunctions appropriate to region 3 are defined by

$$\psi_{3n} = \frac{\cos k_{3n}(y - h_1)}{N_{3n}}, \quad n = 0, 1, 2, \ldots, \tag{3.8}$$

where

$$k_{3n} = \frac{n\pi}{h_2 - h_1}, \quad n = 0, 1, 2, \ldots \tag{3.9}$$

The different form of the eigenvalues in region 3 reflects the fact that the uppermost boundary of that region is a rigid wall, rather than the free surface.

The normalising factors

$$N_{in}^2 = \tfrac{1}{2}\left[1 + \frac{\sin 2k_{in}h_i}{2k_{in}h_i}\right], \quad i = 1, 2, \quad n = 0, 1, 2, \ldots, \tag{3.10}$$

and

$$N_{3n}^2 = \begin{cases} 1, & n = 0 \\ \tfrac{1}{2}, & n > 0 \end{cases} \tag{3.11}$$

have been defined such that

$$\frac{1}{h_i}\int_0^{h_i} \psi_{im}\psi_{in} = \delta_{mn}, \quad i = 1, 2, \tag{3.12}$$

and

$$\frac{1}{h_1 - h_2}\int_{h_2}^{h_1} \psi_{3m}\psi_{3n} = \delta_{mn}, \tag{3.13}$$

where δ_{mn} is the usual Kronecker delta.

The expansions of the symmetric and the antisymmetric parts of the velocity potential in each region are given by

$$\phi^s = \begin{cases} \phi_0 N_{10}\left[\tfrac{1}{2}\,\mathrm{e}^{-\mathrm{i}k_1 x}\psi_{10} + \sum_{n=0}^{\infty} A_{1n}^s\,\mathrm{e}^{-k_{1n}(x-a)}\psi_{1n}\right], & \text{in region 1} \\ \phi_0 N_{10}\sum_{n=0}^{\infty} A_{2n}^s \cosh k_{2n}x\psi_{2n}, & \text{in region 2} \\ \phi_0 N_{10}\left[A_{30}^s\psi_{30} + \sum_{n=1}^{\infty} A_{3n}^s \cosh k_{3n}x\psi_{3n}\right], & \text{in region 3} \end{cases} \tag{3.14}$$

and

$$\phi^a = \begin{cases} \phi_0 N_{10}\left[\tfrac{1}{2}\,\mathrm{e}^{-\mathrm{i}k_1 x}\psi_{10} + \sum_{n=0}^{\infty} A_{1n}^a\,\mathrm{e}^{-k_{1n}(x-a)}\psi_{1n}\right], & \text{in region 1} \\ \phi_0 N_{10}\sum_{n=0}^{\infty} A_{2n}^a \sinh k_{2n}x\psi_{2n}, & \text{in region 2} \\ \phi_0 N_{10}\left[A_{30}^a\frac{x}{a}\psi_{30} + \sum_{n=1}^{\infty} A_{3n}^a \sinh k_{3n}x\psi_{3n}\right], & \text{in region 3} \end{cases} \tag{3.15}$$

The form of the expansions in (3.14) and (3.15) is chosen so that the radiation condition (2.8) is automatically satisfied, on defining

$$R = \left[A_{10}^s + A_{10}^a\right]\mathrm{e}^{-\mathrm{i}k_1 a} \tag{3.16}$$

and

$$T = \left[A_{10}^{s} - A_{10}^{a}\right] \mathrm{e}^{-\mathrm{i}k_1 a}. \tag{3.17}$$

The unknown coefficients, A_{in}^{s} and A_{in}^{a} $(i = 1, 2, 3,\ n = 0, 1, 2, \ldots)$, are determined by ensuring continuity of potential and horizontal velocity on $|x| = a$.

Continuity of ϕ^s on $|x| = a$ requires that

$$\begin{aligned} &\tfrac{1}{2}\,\mathrm{e}^{-\mathrm{i}k_1 a}\psi_{10} + \sum_{n=0}^{\infty} A_{1n}^{s}\psi_{1n} \\ &\quad = \begin{cases} \displaystyle\sum_{n=0}^{\infty} A_{2n}^{s} \cosh k_{2n} a \psi_{2n}, & 0 \leqslant y \leqslant h_2, \\ \displaystyle A_{30}^{s}\psi_{30} + \sum_{n=1}^{\infty} A_{3n}^{s} \cosh k_{3n} a \psi_{3n}, & h_2 \leqslant y \leqslant h_1. \end{cases} \end{aligned} \tag{3.18}$$

Multiplication of (3.18) by the orthonormal set $\{\psi_{2m}(y)\}$ and integration over $(0,\ h_2)$ yields

$$A_{2m}^{s} \cosh k_{2m} a = \tfrac{1}{2}\,\mathrm{e}^{-\mathrm{i}k_1 a} C_{m0} + \sum_{n=0}^{\infty} A_{1n}^{s} C_{mn}, \tag{3.19}$$

where

$$C_{mn} = \frac{1}{h_2} \int_0^{h_2} \psi_{2m}\psi_{1n}\,\mathrm{d}y, \tag{3.20}$$

whilst multiplication of (3.18) by the orthonormal set $\{\psi_{3m}(y)\}$ and integration over $(h_2,\ h_1)$ yields

$$A_{3m}^{s} \cosh k_{3m} a = \tfrac{1}{2}\,\mathrm{e}^{-\mathrm{i}k_1 a} D_{m0} + \sum_{n=0}^{\infty} A_{1n}^{s} D_{mn}, \quad m \neq 0, \tag{3.21}$$

and

$$A_{30}^{s} = \tfrac{1}{2}\,\mathrm{e}^{-\mathrm{i}k_1 a} D_{00} + \sum_{n=0}^{\infty} A_{1n}^{s} D_{0n} \tag{3.22}$$

where

$$D_{mn} = \frac{1}{h_1 - h_2} \int_{h_2}^{h_1} \psi_{3m}\psi_{1n}\,\mathrm{d}y. \tag{3.23}$$

Continuity of $\partial\phi^s/\partial x$ on $|x| = a$ requires that

$$-\frac{ik_1}{2}\,e^{-ik_1 a}\psi_{10} - \sum_{n=0}^{\infty} k_{1n}A_{1n}^s\psi_{1n}$$

$$= \begin{cases} \sum_{n=0}^{\infty} k_{2n}A_{2n}^s \sinh k_{2n}a\psi_{2n}, & 0 \leqslant y \leqslant h_2, \\ \sum_{n=0}^{\infty} k_{3n}A_{3n}^s \sinh k_{3n}a\psi_{3n}, & h_2 \leqslant y \leqslant h_1. \end{cases} \tag{3.24}$$

Multiplication of (3.24) by the orthonormal set $\{\psi_{3m}(y)\}$ and integration over $(0, h_1)$ yields

$$-\tfrac{1}{2}ik_1h_1\,e^{-ik_1a} + ik_1h_1A_{10}^s = \sum_{n=0}^{\infty} k_{2n}h_2A_{2n}^s \sinh k_{2n}aC_{n0}$$

$$+ \sum_{n=1}^{\infty} k_{3n}(h_1 - h_2)A_{3n}^s \sinh k_{3n}aD_{n0} \tag{3.25}$$

and

$$-k_{1m}h_1A_{1m}^s = \sum_{n=0}^{\infty} k_{2n}h_2A_{2n}^s \sinh k_{2n}aC_{nm}$$

$$+ \sum_{n=1}^{\infty} k_{3n}(h_1 - h_2)A_{3n}^s \sinh k_{3n}aD_{nm}, \quad m \neq 0. \tag{3.26}$$

Substitution of A_{2m}^s and A_{3m}^s from (3.19) and (3.21) into (3.25) and (3.26) yields the following system of equations for the A_{1m}^s:

$$A_{1m}^s + \sum_{l=0}^{\infty} \frac{F_{ml}^s}{k_{1m}h_1}A_{1l}^s = -\tfrac{1}{2}\,e^{-ik_1a}\frac{F_{m0}^s}{k_{1m}h_1}, \quad m \neq 0, \tag{3.27}$$

and

$$-iA_{10}^s + \sum_{l=0}^{\infty} \frac{F_{0l}^s}{k_1h_1}A_{1l}^s = -\tfrac{1}{2}\,e^{-ik_1a}\left[\frac{F_{00}^s}{k_1h_1} + i\right] \tag{3.28}$$

where

$$F_{ml}^s = \sum_{n=0}^{\infty} k_{2n}h_2 \tanh k_{2n}aC_{nm}C_{nl} + \sum_{n=1}^{\infty} k_{3n}(h_1 - h_2) \tanh k_{3n}aD_{nm}D_{nl}. \tag{3.29}$$

Continuity of ϕ^a and $\partial\phi^a/\partial x$ on $|x| = a$ requires a second system of equations for the

A^a_{1m} to be satisfied, namely

$$A^a_{1m} + \sum_{l=0}^{\infty} \frac{F^a_{ml}}{k_{1m}h_1} A^a_{1l} = -\tfrac{1}{2}\, \mathrm{e}^{-\mathrm{i}k_1 a} \frac{F^a_{m0}}{k_{1m}h_1}, \quad m \neq 0, \tag{3.30}$$

and

$$-\mathrm{i}A^a_{10} + \sum_{l=0}^{\infty} \frac{F^a_{0l}}{k_1 h_1} A^a_{1l} = -\tfrac{1}{2}\, \mathrm{e}^{-\mathrm{i}k_1 a}\left[\frac{F^a_{00}}{k_1 h_1} + \mathrm{i}\right] \tag{3.31}$$

where

$$F^a_{ml} = \sum_{n=0}^{\infty} k_{2n}h_2 \coth k_{2n}aC_{nm}C_{nl} + \sum_{n=1}^{\infty} k_{3n}(h_1 - h_2) \coth k_{3n}aD_{nm}D_{nl} + \frac{(h_1 - h_2)}{a} D_{0m}D_{0l}. \tag{3.32}$$

The expansions for the radiation potentials ϕ_3 and ϕ_5 are given by

$$\phi_3 = \begin{cases} \displaystyle\sum_{n=0}^{\infty} h_1 A^3_{1n}\, \mathrm{e}^{-k_{1n}(x-a)}\psi_{1n}, & \text{in region 1} \\ \displaystyle\sum_{n=0}^{\infty} h_1 A^3_{2n} \cosh k_{2n}x\psi_{2n} + \left(y - \frac{1}{\kappa}\right), & \text{in region 2} \\ \displaystyle h_1 A^3_{30}\psi_{30} + \sum_{n=1}^{\infty} h_1 A^3_{3n} \cosh k_{3n}x\psi_{3n} + \frac{(y-h_1)^2 - x^2}{2(h_2 - h_1)}, & \text{in region 3} \end{cases} \tag{3.33}$$

and

$$\phi_5 = \begin{cases} \displaystyle\sum_{n=0}^{\infty} h_1^2 A^5_{1n}\, \mathrm{e}^{-k_{1n}(x-a)}\psi_{1n}, & \text{in region 1} \\ \displaystyle\sum_{n=0}^{\infty} h_1^2 A^5_{2n} \sinh k_{2n}x\psi_{2n} + x\left(y - \frac{1}{\kappa}\right), & \text{in region 2} \\ \displaystyle h_1^2 A^5_{30}\frac{x}{a}\psi_{30} + \sum_{n=1}^{\infty} h_1^2 A^5_{3n} \sinh k_{3n}x\psi_{3n} + \frac{3x(y-h_1)^2 - x^3}{6(h_2 - h_1)}, & \text{in region 3} \end{cases} \tag{3.34}$$

where

$$\phi_3(-x, y) = \phi_3(x, y) \tag{3.35}$$

and

$$\phi_5(-x, y) = -\phi_5(x, y), \tag{3.36}$$

since heave oscillations give rise to symmetric motion and roll oscillations to antisymmetric motion. Matching the potentials and horizontal velocity on $x = a$ yields a system of equations for ϕ_3 which has the same matrix but different right-hand side as that for ϕ^s and similarly, a system for ϕ_5 which has the same matrix but different right-hand side as that for ϕ^a.

4. Numerical procedure

The systems of equations for A^s_{1m}, A^a_{1m}, A^3_{1m} and A^5_{1m} are split into their real and imaginary parts and the resulting matrix equations are truncated at a suitable number of terms and solved using a standard NAG library routine, (see e.g. Thomas [16]). It is worth noting that there is little extra expense involved in computing the radiation potentials ϕ_3 and ϕ_5, in addition to the scattering potentials ϕ_s and ϕ_a, because the matrices appearing in the radiation problems are the same as those in the scattering problem.

Care must be taken in performing the summations in (3.29) and (3.32). The quantity C_{nm} has a factor $k^2_{2m} - k^2_{1n}$ in the denominator. For large m, $k_{im} \propto m\pi/h_i$, so the largest term in the first sum in (3.29) occurs when $n = (h_2/h_1)m$ or $(h_2/h_1)l$. The quantity D_{nm} has a factor $k^2_{3m} - k^2_{1n}$ in the denominator and a similar analysis shows that the largest term in the second sum in (3.29) occurs when $n = (h_1 - h_2)m/h_1$ or $(h_1 - h_2)l/h_1$. Each summation must, therefore, be carried out well beyond the Nth term, where for the first sum $N = \max(h_2 m/h_1,\ h_2 l/h_1)$ and for the second $N = \max((h_1 - h_2)m/h_1,\ (h_1 - h_2)l/h_1)$. For fixed values of m and l,

$$k_{2n}k_2 \tanh k_{2n}aC_{nm}C_{nl} = O(n^{-3}) \quad \text{as } n \to \infty$$

and

$$k_{3n}(h_1 - h_2) \tanh k_{3n}aD_{nm}D_{nl} = O(n^{-3}) \quad \text{as } n \to \infty,$$

so that to obtain satisfactory convergence, it is found in practice that the number of terms in each series should be approximately equal to $\max(4N, 20)$. Consideration of the summations in (3.32) yields the same guideline to the number of terms in each sum. A similar analysis was made by Evans and McIver [4] in their work on edge waves.

It should be noted that the substitution of A^s_{20} from (3.19) into (3.21) which yielded a term proportional to $\cot k_2 a$ in F^s_{ml}, is not strictly valid at $k_2 a = (2j + 1)\pi/2$, where j is an integer. Similarly, there is a term in F^a_{ml} proportional to $\cot k_2 a$ which is infinite at $k_2 a = j\pi$. A reformulation of the system of equations is possible that avoids the substitution of A^s_{20} from (3.19) into (3.21) at the expense of increasing the number of unknowns in the system by one. This formulation includes the zero-order equation of (3.19) into the system and solves for A^s_{20} directly. However, in practice, as double-precision arithmetic is used, $k_2 a$ is very rarely close enough to $(2j + 1)\pi/2$ to cause numerical problems in the original system of equations.

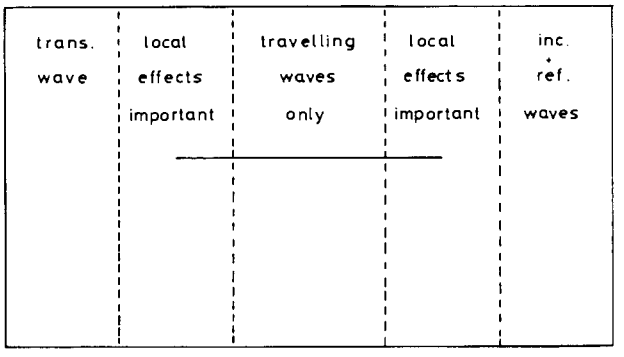

Figure 3. Different flow regions around a long plate.

5. Results and discussion

In Section 3 it was shown that the solution to the scattering and radiation potentials is determined from two, rather complicated, linear systems of equations. In such a case it is desirable, where possible, to check the validity of the numerical work by making comparisons with simple, approximate solutions. One approximation to the full linear solution of the scattering problem may be made when the plate width is large compared to the wavelength. This approximation, which was derived by Newman [12], assumes that there is a region above the plate, far from either end, in which the wavefield consists solely of two plane waves travelling in opposite directions, as illustrated in Figure 3. The amplitudes of these waves together with the reflection and transmission coefficients are determined by a suitable matching with the reflection and transmission coefficients for a semi-infinite plate. If one uses this approximation, the reflection coefficient is given by

$$R = r_+ \, e^{-2ik_1 a} + \frac{r_- t_- t_+ \, e^{2i(2k_2 a - k_1 a)}}{1 - r_-^2 \, e^{4ik_2 a}} \tag{5.1}$$

and the transmission coefficient by

$$T = \frac{t_- t_+ \, e^{2i(k_2 a - k_1 a)}}{1 - r_-^2 \, e^{4ik_2 a}}, \tag{5.2}$$

where $r_\pm$ and $t_\pm$ are the reflection and transmission coefficients obtained when waves are normally incident from either infinity, on a semi-infinite plate. These are available in Heins [7], and (allowing for the difference in notation and correcting a few minor, typographical errors) are given by

$$r_+ = \left[\frac{k_2 - k_1}{k_2 + k_1}\right] \exp(2i\sigma_1), \tag{5.3}$$

$$r_- = \left[\frac{k_1 - k_2}{k_1 + k_2}\right] \exp(-2i\sigma_2), \tag{5.4}$$

$$t_+ = \frac{2k_1}{(k_1+k_2)}\left(\frac{h_1}{h_2}\right)^{1/2}\left[\frac{(k_2h_2)^2-(\kappa h_2)^2}{(k_1h_1)^2-(\kappa h_1)^2}\right]^{1/2}\left[\frac{(k_1h_1)^2+\kappa h_1-(\kappa h_1)^2}{(k_2h_2)^2+\kappa h_2-(\kappa h_2)^2}\right]^{1/2}$$

$$\times \exp \mathrm{i}(\sigma_1-\sigma_2) \tag{5.5}$$

and

$$t_- = \frac{2k_2}{(k_1+k_2)}\left(\frac{h_2}{h_1}\right)^{1/2}\left[\frac{(k_1h_1)^2-(\kappa h_1)^2}{(k_2h_2)^2-(\kappa h_2)^2}\right]^{1/2}\left[\frac{(k_2h_2)^2+\kappa h_2-(\kappa h_2)^2}{(k_1h_1)^2+\kappa h_1-(\kappa h_1)^2}\right]^{1/2}$$

$$\times \exp \mathrm{i}(\sigma_1-\sigma_2) \tag{5.6}$$

where

$$\sigma_1 = -\sum_{n=1}^{\infty}\left[\sin^{-1}\left\{\frac{k_1h_1}{\left[(k_{1n}h_1)^2+(k_1h_1)^2\right]^{1/2}}\right\}-\frac{k_1h_1}{n\pi}\right]$$

$$+\sum_{n=1}^{\infty}\left[\sin^{-1}\left\{\frac{k_1h_2}{\left((k_{2n}h_2)^2+(k_1h_2)^2\right)^{1/2}}\right\}-\frac{k_1h_2}{n\pi}\right]$$

$$+\sum_{n=1}^{\infty}\left[\sin^{-1}\left\{\frac{k_1(h_1-h_2)}{\left[(n\pi)^2+(k_1(h_1-h_2))^2\right]^{1/2}}\right\}-\frac{k_1(h_1-h_2)}{n\pi}\right]$$

$$-\frac{1}{\pi}\left[k_1h_1\ln\left\{\frac{h_1}{h_1-h_2}\right\}+k_1h_2\ln\left\{\frac{h_1-h_2}{h_2}\right\}\right] \tag{5.7}$$

and

$$\sigma_2 = -\sum_{n=1}^{\infty}\left[\sin^{-1}\left\{\frac{k_2h_1}{\left[(k_{1n}h_1)^2+(k_2h_1)^2\right]^{1/2}}\right\}-\frac{k_2h_1}{n\pi}\right]$$

$$+\sum_{n=1}^{\infty}\left[\sin^{-1}\left\{\frac{k_2h_2}{\left[(k_{2n}h_2)^2+(k_2h_2)^2\right]^{1/2}}\right\}-\frac{k_2h_2}{n\pi}\right]$$

$$+\sum_{n=1}^{\infty}\left[\sin^{-1}\left\{\frac{k_2(h_2-h_1)}{\left[(n\pi)^2+(k_2(h_2-h_1))^2\right]^{1/2}}\right\}-\frac{k_2(h_1-h_2)}{n\pi}\right]$$

$$-\frac{1}{\pi}\left[k_2h_1\ln\left\{\frac{h_1}{h_1-h_2}\right\}+k_2h_2\ln\left\{\frac{h_1-h_2}{h_2}\right\}\right]. \tag{5.8}$$

A second approximation based on the first-order, linear, shallow-water theory of Siew and Hurley [15] predicts the reflection coefficient to be

$$|R| = |X||2k_1a \sin 2k_2a - 2\left(\frac{h_2}{h_1}\right)^{1/2}(1 - \cos 2k_2a)| \tag{5.9}$$

where

$$X = \left[\left\{2\left(\frac{h_2}{h_1}\right)^{1/2}(1 - \cos 2k_2a) + 2k_1a\frac{h_1 + h_2}{h_1 - h_2} \sin 2k_2a\right\}\right.$$

$$\left. + 2i\left\{\sin 2k_2a + \frac{2k_2ah_2}{h_1 - h_2} \cos 2k_2a\right\}\right]^{-1}. \tag{5.10}$$

This approximation complements the long-body approximation as illustrated in Figures 4 and 5 where both are compared with the full linear predictions for a plate of non-dimensional submergence depth $h_2/h_1 = 0.1$ and width $a/h_1 = 10$ over two different frequency ranges. As expected, there is good agreement between the shallow-water and full theory over the lower frequency range but the two predictions diverge over the higher frequency range. The converse is true for the long-body approximation.

Figure 6 illustrates the variation in $|R|$ with frequency, for a fixed plate with non-dimensional submergence depth $h_2/h_1 = 0.1$ and plate width $a/h_1 = 0.5$. In order to assess the relative importance of the energy flux above and below the plate, results are also plotted for a rectangular block on the seabed with the same width and height as the plate and for a rectangular block in the surface with the same width and depth as the plate. Both these secondary problems are solved using the method of matched eigenfunction expansions, the details for which follow in an analogous manner to the work already done in this paper. It is apparent that whilst the variation in $|R|$ for the block on the seabed shows the same trend apart from the first zero, as that for the plate, the variation in $|R|$ for the surface block is of markedly different character, being a monotonic increase with

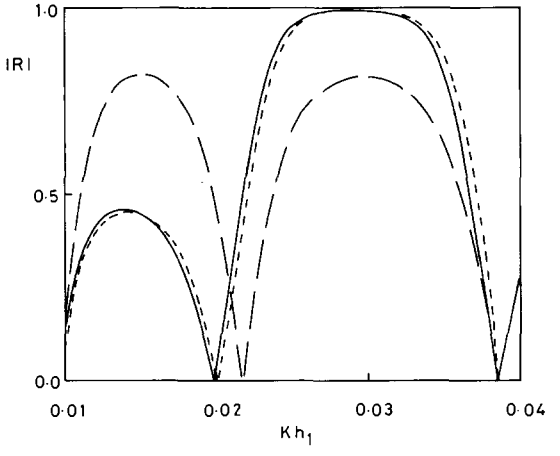

Figure 4. Variation of $|R|$ with wave frequency for $h_2/h_1 = 0.1$ and $a/h_1 = 10$. ———, full linear theory; - - - - - -, shallow-water theory; — — —, long-body approximation.

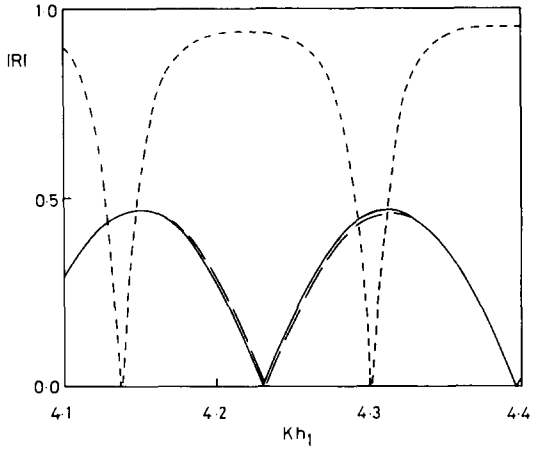

Figure 5. Variation of $|R|$ with wave frequency for $h_2/h_1 = 0.1$ and $a/h_1 = 10.0$. ———, full linear theory; - - - - - -, shallow-water theory; — — —, long-body approximation.

frequency. This suggests that for all but the lowest frequencies the predominant motion is above the plate rather than below. This in itself is perhaps not surprising as the incident-wave motion decays with depth, but a more interesting feature is that at low frequencies ($\kappa h_1 \ll 1$) there is sufficient energy flux beneath the plate to completely change the behaviour of $|R|$.

As previously stated, it is important to determine how the magnitude and phase of the transmitted wave are affected by the plate motion. The far-field form of the total potential is given from (2.8) and (2.15) by

$$\phi \sim \begin{cases} \phi_0\left[A\,\mathrm{e}^{-\mathrm{i}k_1 x} + \left(RA - \mathrm{i}\omega\eta_3 A_3^+ - \mathrm{i}\omega\eta_5 A_5^+\right)\mathrm{e}^{\mathrm{i}k_1 x}\right], & x \to \infty \\ \phi_0\left(AT - \mathrm{i}\omega\eta_3 A_3^- - \mathrm{i}\omega\eta_5 A_5^-\right)\mathrm{e}^{-\mathrm{i}k_1 x}, & x \to -\infty \end{cases} \tag{5.11}$$

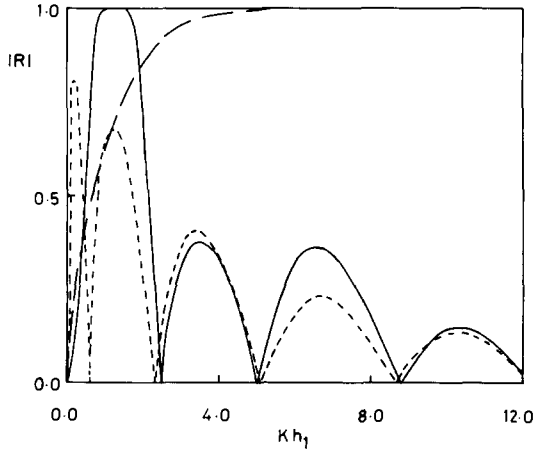

Figure 6. Variation of $|R|$ with wave frequency for a plate, ———; a block on the seabed, - - - - - -; and a block in the surface, — — —. In each case, $h_2/h_1 = 0.1$ and $a/h_1 = 0.5$.

where

$$\phi_0 = -\frac{i\omega \cosh k_1(y-h_1)}{k_1 \sinh k_1 h_1}. \tag{5.12}$$

Various two-dimensional relations between the radiation and scattering problems may be deduced (Mei [10]), namely, the Haskind relations

$$\chi_\alpha = -\frac{\rho g^2 D A A_\alpha^+}{\omega}, \tag{5.13}$$

where

$$D = \tanh k_1 h_1 + k_1 h_1 \operatorname{sech}^2 k_1 h_1, \tag{5.14}$$

the Newman relations,

$$A_\alpha^+ - R(A_\alpha^+)^* - T(A_\alpha^-)^* = 0, \tag{5.15}$$

where * denotes complex conjugate, and the relations between the damping coefficients and the energy in the radiated waves,

$$b_\alpha = \frac{\rho g^2 D}{2\omega}\left(|A_\alpha^+|^2 + |A_\alpha^-|^2\right). \tag{5.16}$$

It follows, using the equations of motion for η_α, (2.19), and the symmetry of the geometry which yields

$$A_3^- = A_3^+ \tag{5.17}$$

and

$$A_5^- = -A_5^+, \tag{5.18}$$

that (5.11) may be written as

$$\phi \sim \begin{cases} \phi_0 A\left[e^{-ik_1 x} + e^{ik_1 x}\left\{R + \dfrac{i\omega b_3(R+T)}{-\omega^2(m_3+a_3)+c_3-i\omega b_3} + \dfrac{i\omega b_5(R-T)}{-\omega^2(m_5+a_5)+c_5-i\omega b_5}\right\}\right], & x \to \infty, \\ \phi_0 A\, e^{-ik_1 x}\left\{T + \dfrac{i\omega b_3(R+T)}{-\omega^2(m_3+a_3)+c_3-i\omega b_3} - \dfrac{i\omega b_5}{-\omega^2(m_5+a_5)+c_5-i\omega b_5}\right\}, & x \to -\infty. \end{cases} \tag{5.19}$$

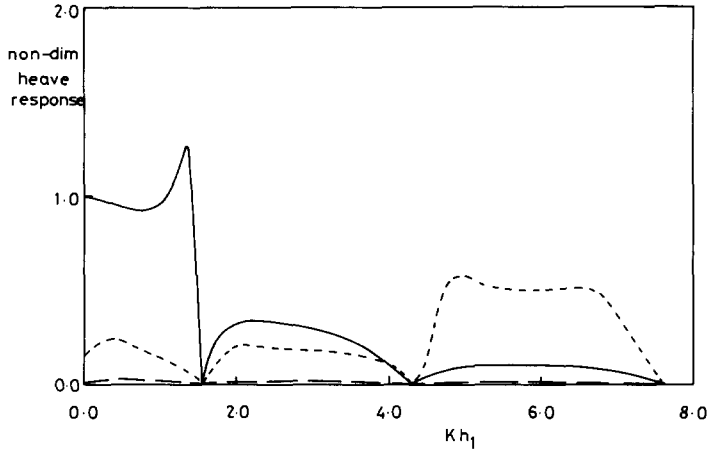

Figure 7. Variation of the amplitude of the heave response with frequency for $h_2/h_1 = 0.1$ and $a/h_1 = 1.0$. ———, neutrally buoyant plate; - - - - - -, $s_3 = 10$; — — —, $s_3 = 100$.

It is of interest to examine analytically the case in which the stiffness is chosen such that $c_\alpha = \omega^2(m_\alpha + a_\alpha)$, $\alpha = 3, 5$. The far-field form of the total potential at the frequency at which this is valid is given by

$$\phi \sim \begin{cases} \phi_0 A(e^{-ik_1 x} - Re^{ik_1 x}), & x \to \infty \\ \phi_0 A(-T)\, e^{-ik_1 x}, & x \to -\infty \end{cases} \tag{5.20}$$

that is, the diffracted waves have the same magnitude but are 180° out of phase with what they would be if the plate were held fixed. This has important consequences as it provides a mechanism whereby, without changing the position and size of the plate, the phase shift in the transmitted wave may be altered by merely varying the stiffness of the mooring cables. A word of caution should be added here. The response motions of the plate, from (2.19) are

$$\eta_\alpha = \frac{\chi_\alpha}{c_\alpha - \omega^2(m_\alpha + a_\alpha) - i\omega b_\alpha}, \quad \alpha = 3, 5. \tag{5.21}$$

If the stiffness in the cables is chosen such that $c_\alpha = \omega^2(m_\alpha + a_\alpha)$ and the damping b_α is small, it is clearly possible to induce large motions in the plate, thus violating one of the assumptions on which this linearised theory is based.

Figures 7 and 8 illustrate the effect of varying the stiffness and position of attachment of the cables on the heave and roll response of a plate with non-dimensional submergence depth $h_2/h_1 = 0.1$ and width $a/h_1 = 1.0$. The stiffness parameter in the figure captions, s_α, is defined by

$$s_3 = \frac{c_3}{\rho a g} \tag{5.22}$$

and

$$s_5 = \frac{c_5}{\rho a^3 g}. \tag{5.23}$$

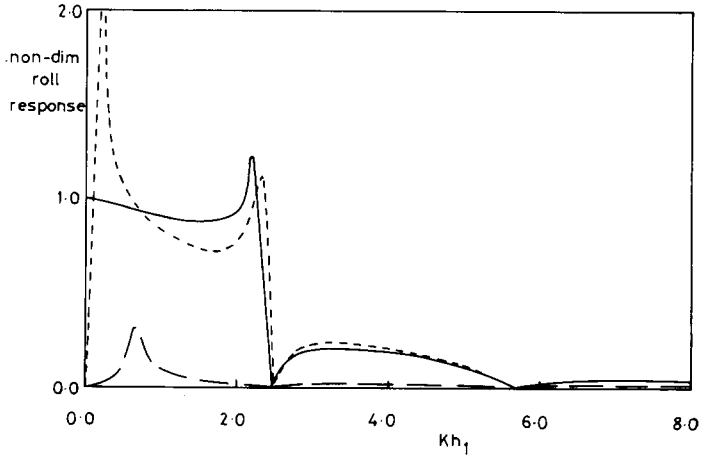

Figure 8. Variation of the amplitude of the roll response with frequency for $h_2/h_1 = 0.1$ and $a/h_1 = 1.0$. ———, neutrally buoyant plate; - - - - - -, $s_5 = 1.0$; — — —, $s_5 = 9.0$.

The heave response is non-dimensionalised by the vertical-displacement amplitude of a water particle in the incident wave with mean depth equal to that of the plate. Similarly, the roll response is non-dimensionalised by the maximum steepness of the incident wave motion at that depth. Thus the non-dimensionalised responses of a neutrally buoyant plate, which should move with the waves at low frequency, should tend to 1.0 as Kh_1 tends to zero, as indeed shown in Figures 7 and 8. In the calculations, the mass of the plate is taken as zero in order to be consistent with the assumption that the plate is infinitely thin. In practice, although this is clearly not true, it is a reasonable approximation as the mass of the plate would generally be much smaller than its added mass. From the figures, it may be seen that if the plate is moored by very stiff cables, the motion is much reduced from the neutrally buoyant case whereas the choice of an intermediate stiffness parameter enables the responses motions to be larger than those of the neutrally buoyant plate over part of the frequency range. The zeros in the heave response are associated with the zeros in the vertical exciting force and approximately correspond to the frequencies at which $2a/\lambda_2 = n$, $n = 1, 2, \ldots$, where λ_2 is the wavelength over the plate. This is not surprising because when the plate width is an integral number of wavelengths, the contributions to the vertical force, considering the flow field above the plate only, cancel each other out when integrated over the top surface of the plate. It is not so clear how to interpret the zeros in the roll response except to say that they are associated with the zeros in the roll exciting moment.

Ideally it would be desirable to have a plate and mooring system for which the reflection coefficient were zero and it were possible to choose the phase of the transmitted wave arbitrarily. Clearly this would be impossible, but it is necessary that the reflection coefficient should be small. Otherwise the aim of the water-wave lens, which is to concentrate the wave energy at one particular point, would be defeated. Figures 9, 11, 13 and 15 illustrate the variation of the amplitude of the total reflection coefficient with wave frequency for a number of plates with different widths, submerged at the same depth, $h_2/h_1 = 0.1$. Figures 10, 12, 14 and 16 show the corresponding phase of the transmitted wave, given between $+$ and $-\pi$. In each case the reflection coefficient has been plotted for a fixed plate ($c_\alpha/[\omega^2(m_\alpha + a_\alpha)] \gg 1$, $\alpha = 3, 5$), a neutrally buoyant plate ($c_\alpha/[\omega^2(m_\alpha + a_\alpha)] = 0$, $\alpha = 3, 5$), and a plate with cables of medium stiffness. In each of the figures it

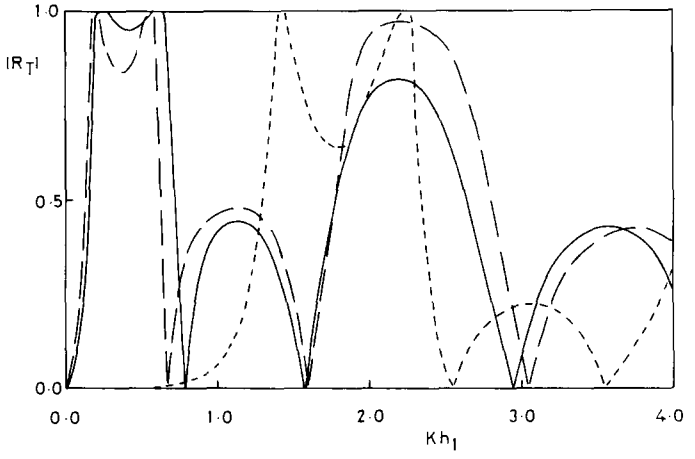

Figure 9. Variation of the amplitude of the total reflection coefficient with wave frequency for $h_2/h_1 = 0.1$ and $a/h_1 = 1.0$. ———, fixed plate; - - - - - -, neutrally buoyant plate; — — —, $s_3 = 10.0$ and $s_5 = 5.0$.

is clear that the neutrally buoyant plate reflects very little of the incident wave over the lowest part of the frequency range. Unfortunately, this is coupled with an almost zero phase lag in the transmitted wave which means that the plate does not affect the wave field much at all in this frequency range. In fact, it may be seen from the figures that whatever the stiffness of the cables, it is necessary that Kh_1 should be greater than the value at which the first maximum is the reflection coefficient occurs before it is possible to obtain an appreciable phase lag in the transmitted wave coupled with a small reflection coefficient. In practical terms this means that the plate width should be at least half to one times the incident wavelength. Figure 9 shows that this is not a sufficient condition, however, as there are further large peaks in the reflection coefficient after the first maximum. Care must therefore be taken to ensure that the frequency range of interest is known before the configuration of the plate and mooring system is chosen.

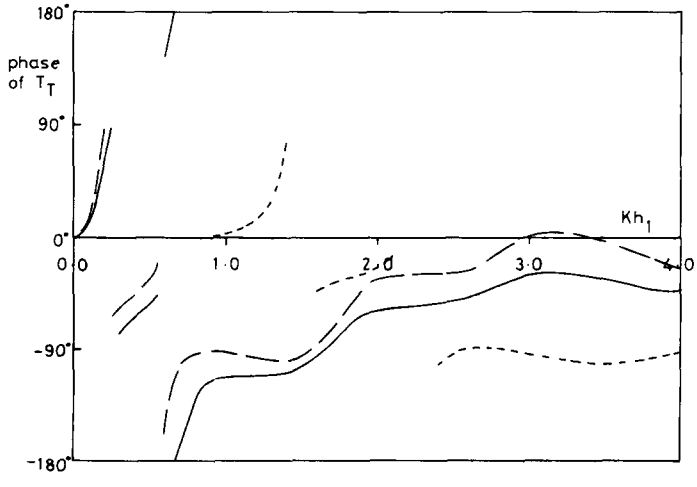

Figure 10. Variation of the phase of the total transmitted wave with wave frequency for $h_2/h_1 = 0.1$ and $a/h_1 = 1.0$. ———, fixed plate; - - - - - -, neutrally buoyant plate; — — —, $s_3 = 10.0$ and $s_5 = 5.0$.

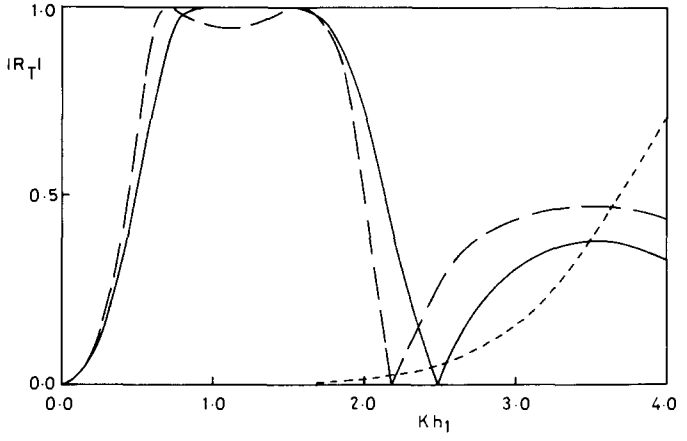

Figure 11. Variation of the amplitude of the total reflection coefficient with wave frequency for $h_2/h_1 = 0.1$ and $a/h_1 = 0.5$. ———, fixed plate; - - - - - -, neutrally buoyant plate; — — —, $s_3 = 10.0$ and $s_5 = 5.0$.

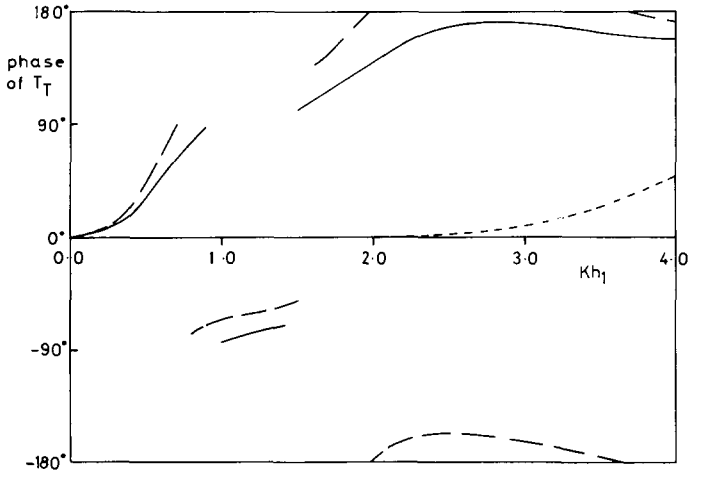

Figure 12. Variation of the phase of the total transmitted wave with frequency for $h_2/h_1 = 0.1$ and $a/h_1 = 0.5$. ———, fixed; - - - - - -, neutrally buoyant; — — —, $s_3 = 10.0$ and $s_5 = 5.0$.

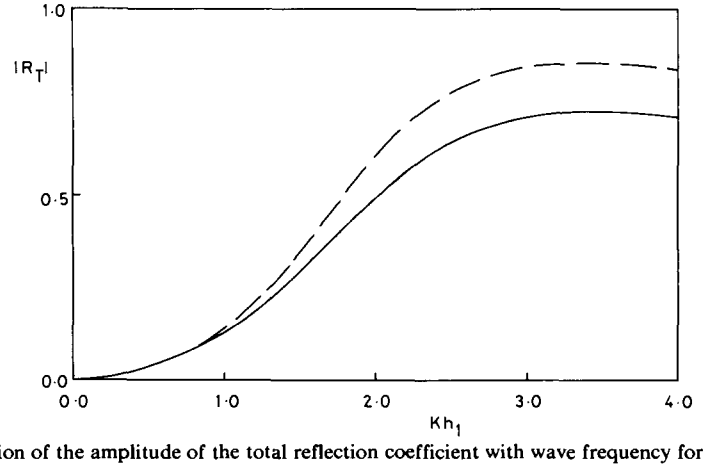

Figure 13. Variation of the amplitude of the total reflection coefficient with wave frequency for $h_2/h_1 = 0.1$ and $a/h_1 = 0.2$. ———, fixed plate; - - - - - -, neutrally buoyant; — — —, $s_3 = 10.0$ and $s_5 = 5.0$.

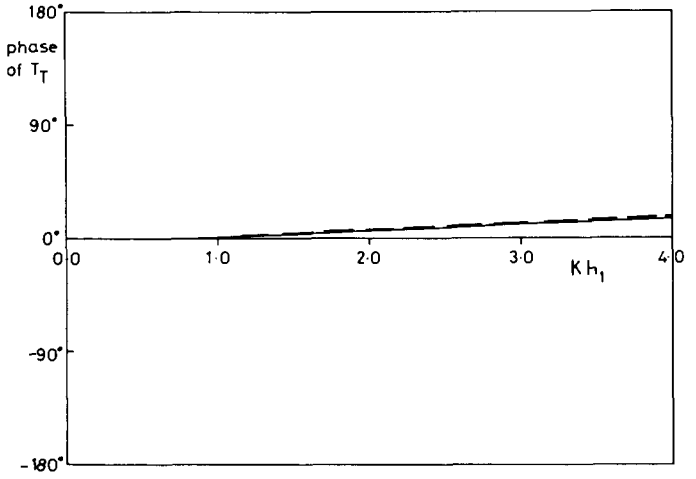

Figure 14. Variation of the phase of the total transmission coefficient with wave frequency for $h_2/h_1 = 0.1$ and $a/h_1 = 0.2$. ———, fixed plate; - - - - - -, neutrally buoyant; — — —, $s_3 = 10.0$ and $s_5 = 5.0$.

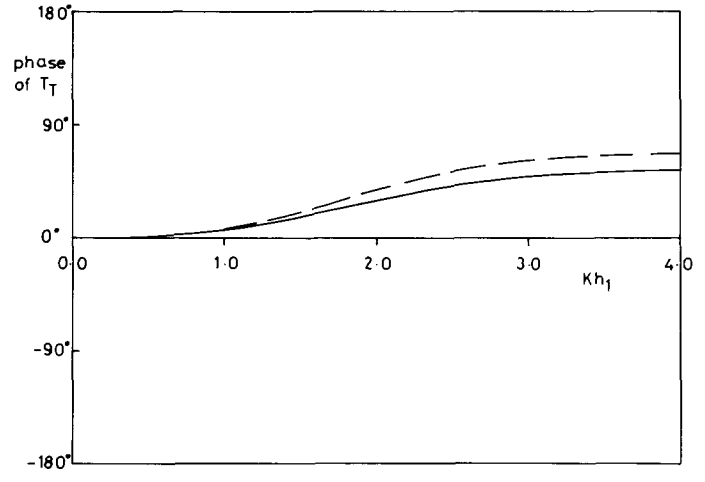

Figure 15. Variation of the amplitude of the total reflection coefficient with wave frequency for $h_2/h_1 = 0.1$ and $a/h_1 = 0.1$. ———, fixed plate; - - - - - -, neutrally buoyant; — — —, $s_3 = 10.0$ and $s_5 = 5.0$.

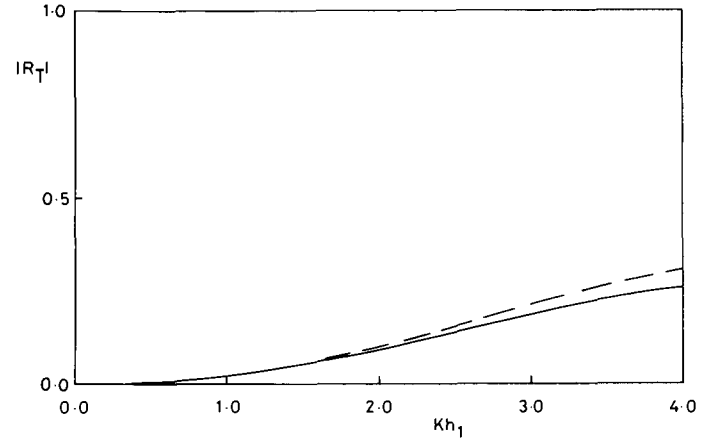

Figure 16. Variation of the phase of the total transmission coefficient with wave frequency for $h_2/h_1 = 0.1$ and $a/h_1 = 0.1$. ———, fixed plate; - - - - - -, neutrally buoyant plate; — — —, $s_3 = 10.0$ and $s_5 = 5.0$.

6. Conclusion

A Norwegian research group has demonstrated that a water-wave lens may be constructed out of a system of underwater structures. In this work we considered modelling one of these structures by a horizontal flat plate which is moored to the seabed. Numerical results for the full linear theory were checked against both a shallow-water and a long-body approximation and good agreement was obtained over each of their respective ranges of validity. A comparison was also made with the results for a fixed block on the seabed with the same height and width as the plate and for a fixed block in the surface with the same depth and width as the plate. The variation of the reflection coefficient for the block on the seabed showed the same trend, except at low frequencies, as that for the plate whilst that for the block in the surface was of markedly different character indicating that the wave motion was predominantly above the plate.

The effect of the moorings on the response motions of the plate was examined and it was observed that whilst very stiff cables considerably reduced the motion of the plate from what it would be if it were neutrally buoyant, it was possible, by choosing an intermediate stiffness parameter, for the response motion to be larger than that for the neutrally buoyant plate over part of the frequency range. It was also observed that the heave response of the plate was zero when the plate width was approximately an integral number of wavelengths (referring to the wavelength over the plate) independent of the choice of stiffness of the cables.

The effect of varying the mooring stiffness on the far-field form of the total potential was also examined and it was shown that by choosing the stiffness such that $c_\alpha = \omega^2(m_\alpha + a_\alpha)$, $\alpha = 3, 5$, both the total reflection and total transmission coefficients were 180° out of phase with what they would be for a fixed plate. Results were presented illustrating the variation of the amplitude of the total reflection coefficient and also the phase of the transmission coefficient with frequency and it was found that a necessary condition to obtain a small reflection coefficient coupled with an appreciable phase change in the transmission coefficient, was that the plate width should be at least half to one times the incident wavelength.

Acknowledgements

The author would like to thank Drs D.V. Evans and P. McIver for many helpful discussions during the preparation of this work. Financial support was provided by S.E.R.C. in conjunction with N.M.I. Ltd. under the case studentship scheme.

References

[1] J.E. Burke, Scattering of surface waves on an infinitely deep fluid, *J. Mathematical Physics* 5 (1964) 805–819.

[2] W.R. Dean, On the reflection of surface waves by a submerged circular cylinder, *Proc. Camb. Phil. Soc.* 44 (1948) 483–491.

[3] D.V. Evans, Power from water waves, *Annual Review of Fluid Mechanics* 13 (1981) 157–187.

[4] D.V. Evans and P. McIver, Edge waves over a shelf: full linear theory, *J. Fluid Mech.* 142 (1984) 79–95.

[5] T.R. Greene and A.E. Heins, Water waves over a channel of infinite depth, *Quarterly J. of Applied Maths.* 11 (1953) 201–214.

[6] J. Grue and E. Palm, Reflection of surface waves by submerged cylinders, *Applied Ocean Research* 6 (1984) 54–60.
[7] A.E. Heins, Water waves over a channel of finite depth with a submerged plane barrier, *Canadian Journal of Maths.* 2 (1950) 210–222.
[8] E. Mehlum, A circular cylinder in water waves, *Applied Ocean Research* 2 (1980) 171–177.
[9] E. Mehlum and J.J. Stamnes, On the focusing of ocean swells and its significance in power production, Central Inst. for Indust. Res., Blindern, Oslo, SI Rep. 77 01 38 (1978).
[10] C.C. Mei, *The Applied Dynamics of Ocean Surface Waves,* Wiley-Interscience, New York (1983).
[11] C.C. Mei and J.L. Black, Scattering of surface waves by rectangular obstacles in water of finite depth, *J. Fluid Mech.* 38 (1969) 499–511.
[12] J.N. Newman, Propagation of water waves past long two-dimensional obstacles, *J. Fluid Mech.* 23 (1965) 23–29.
[13] M. Patarapanich, Maximum and zero reflection from a submerged plate. *J. Waterway, Port, Coastal and Ocean Engineering* 110 (1984) 171–181.
[14] M. Patarapanich, Forces and moment on a horizontal plate due to wave scattering, *Coastal Engineering* 8 (1984) 279–301.
[15] P.F. Siew and D.G. Hurley, Long surface waves incident on a submerged horizontal plate, *J. Fluid Mech.* 83 (1977) 141–151.
[16] J.R. Thomas, The hydrodynamics of certain wave energy absorbers, Ph.D. Thesis, University of Bristol (1981).
[17] F. Ursell, Surface waves on deep water in the presence of a submerged cylinder, *Proc. Camb. Phil. Soc.* 46 (1950) 141–158.
[18] J.V. Wehausen and E.V. Laitone, Surface waves, *Handbuch der Physik* 9 (1960) 446–778.